Observation of Non-vanishing Optical Helicity in Thermal Radiation from Symmetry-Broken Metasurfaces

Xueji Wang*,† Tyler Sentz*,† Sathwik Bharadwaj,† Subir Ray,† Yifan Wang,† Dan Jiao,† Limei Qi,‡ and Zubin Jacob*,†

†*Elmore Family School of Electrical and Computer Engineering, Purdue University, West Lafayette, Indiana, 47907, USA*

‡*School of Electronic Engineering, Beijing University of Posts and Telecommunications, Beijing, 100876, China*

E-mail: zjacob@purdue.edu

*These authors contribute equally to this work

Abstract

Thermal radiation is traditionally an incoherent radiative signal, where the radiated heat is highly unpolarized, spectrally broad, and omnidirectional. The recent extensive interests in thermal photonics focus on tailoring the temporal coherence (spectrum) and spatial coherence (directivity) of thermal radiation. Here, we investigate the photon spin characteristics of the radiation excited by thermal fluctuations using a symmetry-broken metasurface. Utilizing spin-polarized angle-resolved thermal emission spectroscopy (SPARTES), we explicitly show when both mirror- and inversion- symmetries are broken, the summation of spin-angular momentum projected on wavevectors, namely the optical helicity, can be non-vanishing even without applying a magnetic

field. We find the photon spin and the energy-momentum dispersion of thermal radiation can be effectively tailored through symmetry engineering. Our results firmly suggest the symmetry-based strategy provides a general pathway for comprehensively controlling the temporal, spatial, and especially spin coherence of thermal radiation.

Main

Thermal radiation describes the universal phenomenon that all objects at non-zero temperatures emit infrared electromagnetic energy.[1] Controlling this omnipresent radiative energy source is of vital importance for various modern world applications,[2] ranging from thermophotovoltaics,[3–5] radiative cooling,[6,7] to novel information-processing devices[8,9] and optical gas sensing.[10] Looking at the recent efforts on controlling thermal radiation, significant progress has been made in tailoring its temporal coherence, i.e. spectrum,[11,11–15] and the spatial coherence, i.e. directivity.[16,17] However, the photon spin, as another crucial characteristic of electromagnetic radiation, is so far commonly ignored, due to the fact that conventional thermal emitters show weak to zero spin-angular momentum (SAM).

Nevertheless, the photon spin, especially its intertwined characteristics with spectrum and directivity, can bring in a brand new degree of freedom for tailoring thermal radiation. Fundamental obstacles arise from the fact that thermal radiation is substantially determined by the Bose-Einstein distribution of photons. The statistical behavior of thermal photons indicates thermal radiation is commonly incoherent and spin degenerated. Surprisingly, it has been observed that some astronomical objects in nature show observable SAM. This unique phenomenon has drawn increasing attention as it contains exclusive information about the universe and is regarded as a possible signature of life. However, the fundamental mechanism of these observations is either the filtering by chiral molecules[18] or the existence of a strong magnetic field.[19] They are not ideal pathways for practical applications, and thus not of general interest to the subject of thermal radiation engineering.

Besides, recent studies reveal that the thermal radiation from topological insulators[20,21] and Weyl semimetals[22] exhibits circularly polarized characteristics. This is a manifestation of the microscopic mechanisms where the fluctuation-driven torque is generated under magnetic fields. As a result, macroscopically, it is expected the circularly polarization can be omnidirectional in the far field. In other words, the summation of SAM projected on wavevectors, namely the optical helicity, can be non-zero in these cases. However, complicated material systems or high magnetic fields are required here to break the time-reversal symmetry. Until now, there is no direct demonstration of non-vanishing optical helicity in a time-reversal symmetry preserved system.

To overcome this, we consider the fundamental constraints and opportunities for spin-degeneracy removal from a symmetry point of view. We investigate here pseudo-2D systems under time-reversal symmetry. Firstly, assuming inversion- and mirror- symmetry are both preserved, the spin degenerates, and no circularly polarized radiation can be observed as illustrated in Fig.1e. Secondly, by breaking the inversion symmetry, an anti-symmetric spin characteristic can be observed.[23] However, we emphasize that although circularly polarized thermal radiation can be generated in this scenario, it only occurs in oblique directions, as the mirror-symmetry guarantees spin degenerates in the surface normal. The anti-symmetric spin pattern ensures the total optical helicity is zero (Fig.1f). Lastly, we show that by further breaking the mirror-symmetry, an extra k term can exist, which releases all the constraints and make asymmetric spin characteristics and non-vanishing optical helicity possible (Fig.1g).

Based on the symmetry analysis, in this work, we show an experimental realization of the symmetry-broken metasurface with removed spin degeneracy, generating magnetic-field-free circular-polarized thermal radiation with a degree of circular-polarization (DoCP) exceeding 0.6. To reveal the energy-momentum dispersion and the corresponding spin characteristics in the thermal radiation, we establish a unique spin-polarized angle-resolved thermal emission spectroscopy (SPARTES) system, overcoming the limitations of conventional thermal emission spectroscopy where the measurements are limited to the proximity of surface-normal

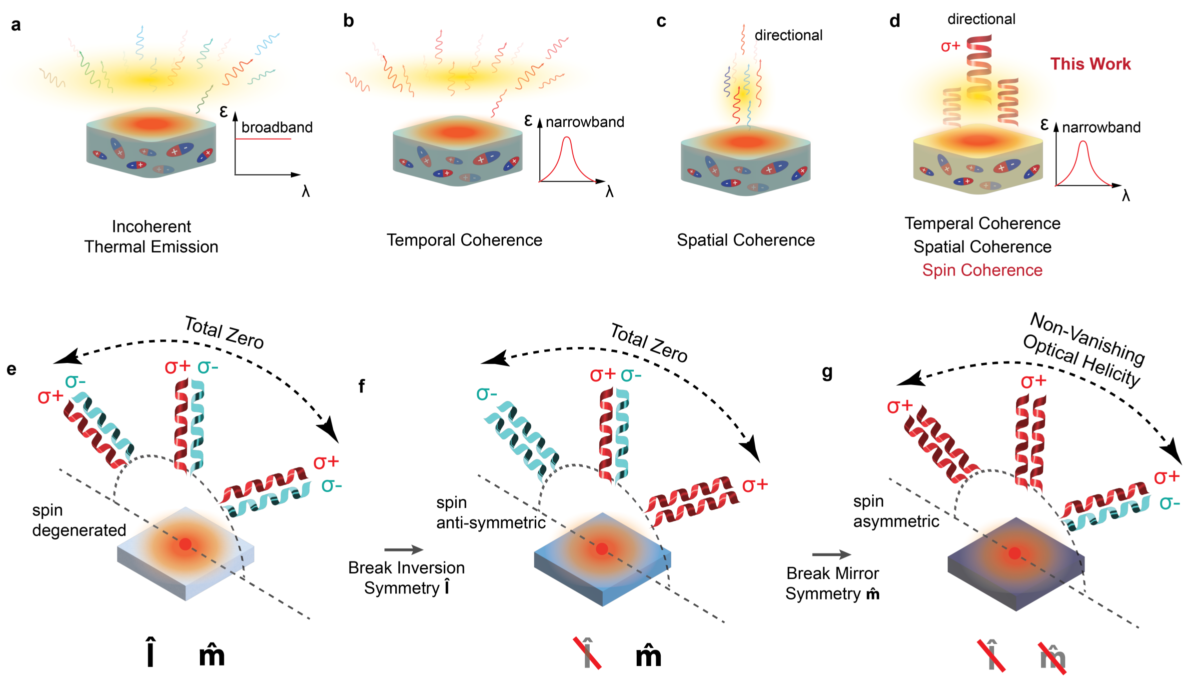

Figure 1: **a-d.** Various aspects of thermal emission engineering. In this work, by adding the optical spin control, we achieve comprehensive tailoring of thermal emission. **e-g.** Schematics demonstrating the constraints of spin degeneracy removal from symmetries. The non-vanishing optical helicity can only be observed when both inversion- and mirror- symmetries are broken (g)

direction. Based on a thorough characterization, we show an omnidirectional high DoCP and spin asymmetry at a remarkable dispersionless band around 7μm. Particularly, we directly observe a non-zero total optical helicity in thermal radiation, which originates from the breaking of mirror symmetry. We emphasize this is fundamentally prohibited in previous studies, where mirror symmetry is preserved and the spin characteristics are thus anti-symmetric in k-space. The complete symmetry breaking also provides full freedom to introduce new symmetries when used as constitutive building blocks. As some examples, we discuss later three representative configurations with mirror, inversion, and four-fold rotational (C4) symmetries, and show that thermal radiation can be significantly altered by the symmetries. With this symmetry-based approach, we provide a general and effective pathway to comprehensively engineering the spectral, spatial, and spin characteristics of thermal radiation.

Circularly Polarized Thermal Radiation

To show the non-vanishing optical helicity, we start by demonstrating the spin degeneracy is removed in our symmetry-broken metasurface and the far-field thermal radiation is significantly circular-polarized at 7µm. A schematic of the metasurface is shown in Fig 2a, where a rectangular array of F-shaped meta-atoms is patterned on a SiO2 dielectric layer with a gold backplane. The measured emissivity of left-handed circular-polarized light (LCP) is more than 4 times larger than the emissivity of right-handed circular-polarized light (RCP) at the surface normal direction as shown in Fig 2b, which is in good agreement with our simulation results. In Fig 2c, we show a complete characterization of the polarization state based on Stokes parameters, where S_1 and S_2 reveal the degree and the direction of linear polarization, and S_3 is equivalent to the DoCP. We emphasize that at the peak wavelength of 7µm, although the DoCP is below 0.7, the thermally-excited photons are still in highly circularly polarized eigenstates because of the near-zero S_1 and S_2. The polarization state can be represented by a circular area that is centered close to the north pole of the Poincare sphere (inset of Fig 2c). The relatively limited DoCP is actually from the limited coherence of the thermal emission signal.

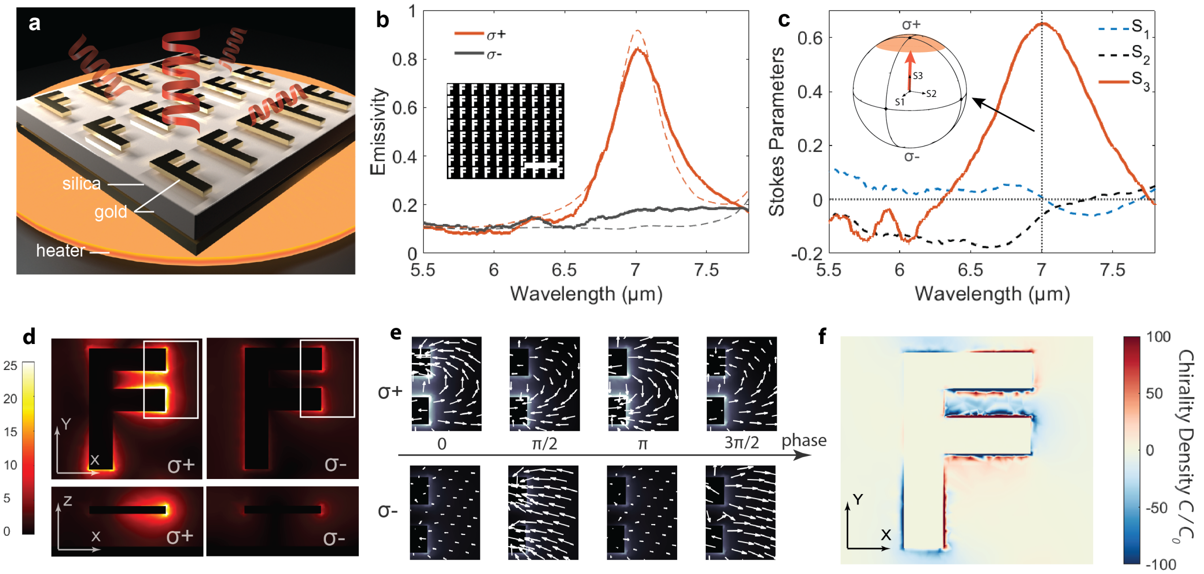

Figure 2: **a.** Schematic of the symmetry-broken metasurface with F-shape meta-atoms. **b.** The measured LCP ($\sigma+$) and RCP ($\sigma-$) emissivity (solid) of the fabricated devices, which show good agreement with the simulation results (dashed). Inset: SEM imaging of the fabricated device. **c.** Stokes parameters show the full polarization state. Inset: representation of the polarization state in the Poincare sphere. **d.** The time-averaged electric field strength (normalized by the field E_0 of incident waves) at 7µm under LCP (left) and RCP (right) excitations. The fields are plotted along the XY (top) and XZ (bottom) planes, respectively. **e.** Evolution of the vector electric field is plotted for the boxes in d. The field is significantly circularly polarized under LCP excitation (top), while it is more linearly polarized under RCP excitation (bottom). **f.** The local optical chirality density C, normalized by C_0 of the incident LCP.

To show the microscopic mechanisms of the cicular polarization and non-vanishing optical helicity, we investigate the near-field electromagnetic response of the metasurface. Fundamentally speaking, the mechanisms of spin degeneracy removal in photonic systems can be divided into two categories. On the one hand, the Pancharatnam-Berry phase generated by a geometric gradient can lead to spin-dependent photon behaviors.[24,25] On the other hand, the phenomenon can also originate from the intrinsic local chirality in the meta-atoms.[26,27] We reveal that the strong intrinsic local chirality of our F-shaped plasmonic meta-atoms is the origin of the observed circular-polarized thermal radiation in the far-field. To start with, we calculate the electric field distribution using the finite element method (FEM). The normalized electric field strength at 7µm under LCP and RCP excitations are plotted in Fig 2d. An evident resonant enhancement can be observed for LCP excitation near the region of the two horizontal lines of 'F', while the enhancement is clearly absent for RCP excitation. Obviously, the spin-selective resonance is the direct reason for the LCP emissivity peak at 7µm. For more insights, we plot in Fig 2e the temporal evolution of the electric field polarization around the strong-field region. The electric field is predominantly circular-polarized under LCP excitation, where it is mainly the direction of the polarization vector that is evolving with phase. In contrast, under RCP excitation, the magnitude of polarization is oscillating, which reveals the field is predominantly linearly polarized. We argue that the circularly polarized near-field indicates the high absorption and thus strong emission of LCP, while the linearly polarized near-field corresponds to weak emission of RCP. We use optical chirality density C as the metrics to quantitatively characterize the circular-polarized feature of the near-field,[28] as $C \equiv \frac{\varepsilon_0}{2}\mathbf{E} \cdot \nabla \times \mathbf{E} + \frac{1}{2\mu_0}\mathbf{B} \cdot \nabla \times \mathbf{B}$, where $\mathbf{E}$ and $\mathbf{B}$ are the time-dependent electric and magnetic fields, and ε_0 and μ_0 are the permittivity and permeability of vacuum. We emphasize that the local chirality is two orders of magnitude larger than the chirality of the incident LCP as shown in Fig 2f. The super-chiral near-field under LCP excitation is a manifestation of a strong LCP absorption/emission, and at the same time indicates the intrinsic local chirality is the dominant mechanism for our observation of circular-polarized thermal radiation.

Spin-Polarized Angle-resolved Thermal Emission Spectroscopy

To demonstrate the non-vanishing optical helicity and map the energy-momentum ($E - k$) dispersion of thermal radiation, we establish a unique SPARTES system. The system allows

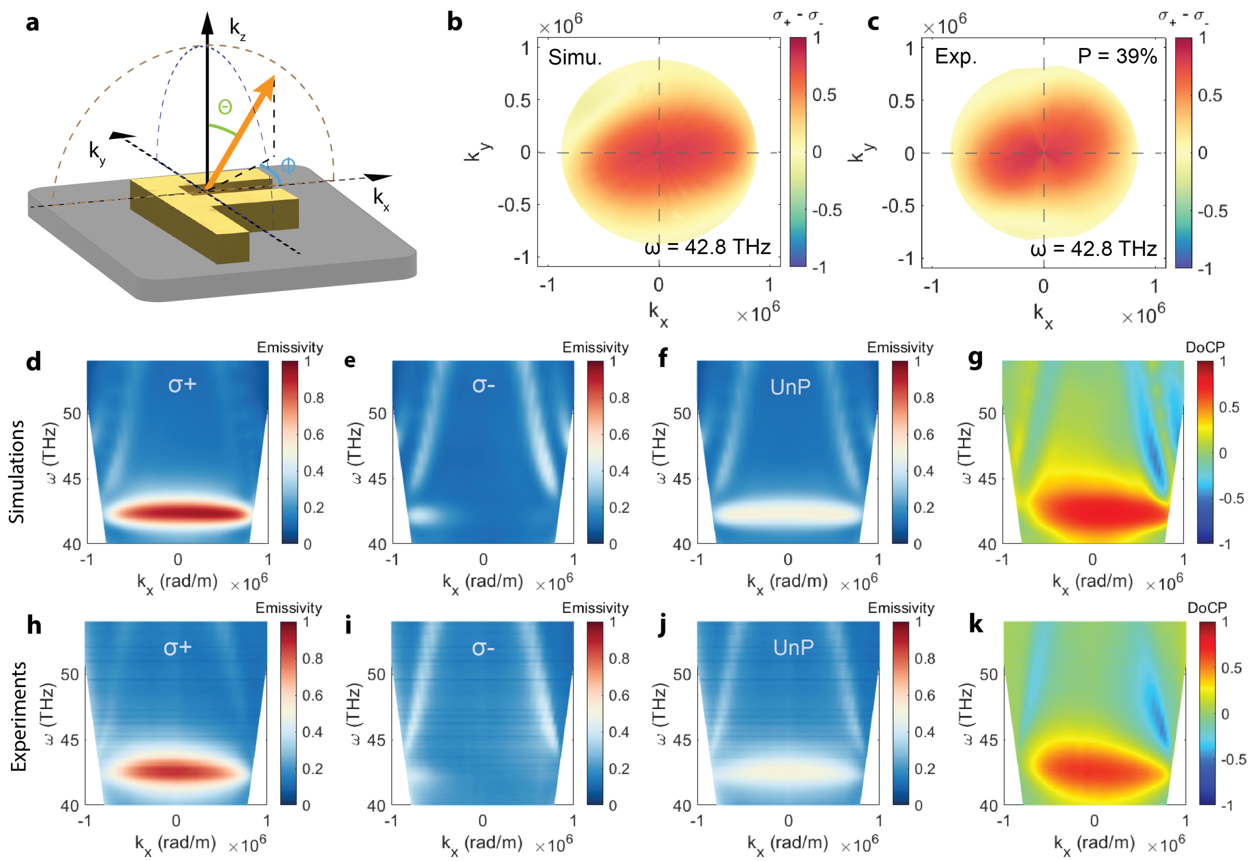

Figure 3: Spin-polarized angle-resolved thermal emission spectroscopy (SPARTES) **a.** Schematic of the coordinate system. **b-c.** Calculated (b) and experimentally measured (c) differential emissivity at 7 microns. The thermal radiation is predominantly LCP over the entire hemisphere. The total optical helicity, which is proportional to the integral of the differential emissivity in the k-space, is non-zero. It reaches more than one third of the fundamental limits (P=39%). **d-k.** Simulated (top) and measured (bottom) angle-resolved thermal radiation spectra in the energy-momentum space. The LCP emissivity (d, h), RCP emissivity (e, i), unpolarized emissivity (f, j), and DoCP (g, k) are plotted for comparison. A unique spin-polarized dispersionless band and the spin asymmetry can be clearly observed.

us to characterize the spectral and polarimetric properties of thermal radiation signals at all azimuth (ϕ) and deflection angles (θ) over the entire far-field hemisphere as shown in Fig.3 a. (The detailed description of the SPARTES system and full thermal emission spectroscopy data can be seen in supplementary section II.) In the following, we take the experimental data along k_x for our discussion ($k_y = 0$). The measured spectra are plotted in Fig.3 g-j and show an excellent agreement with simulations (Fig.3 c-f). A strong contrast between the emissivity of LCP and RCP can be observed, which is a direct manifestation of the spin degeneracy removal. Despite the LCP and RCP emissivities being asymmetric in $+k$ and $-k$ by themselves, we note that there is a clear symmetric pattern of the averaged emissivity ($\sigma_+/2+\sigma_-/2$). This is because the averaged emissivity is proportional to the total radiative power, and the symmetric total radiation in k-space is fundamentally guaranteed by the time-reversal symmetry in this magnetic-field-free system. The asymmetric LCP and RCP emissivity also leads to a unique DoCP pattern, which is neither symmetric nor anti-symmetric. Here, the DoCP is defined as $(\sigma_+ - \sigma_-)/(\sigma_+ + \sigma_-)$, which is +1 for LCP, -1 for RCP, and 0 for spin-degenerated radiation. We point out that this spin asymmetry in k-space is from the complete symmetry breaking of our 'F' structure, where neither the 2D inversion-symmetry nor the mirror-symmetry is preserved.

Interestingly, we observe that the strong thermal emission at 7µm is from a dispersionless energy band along k_x. To reveal the thermal radiation characteristics in this dispersionless energy band, we plotted the differential circular-polarized emissivity ($\sigma_+ - \sigma_-$) at 7µm on the entire hemisphere (projected onto the k_{xy} plane). As evidently illustrated in Fig. 2b, the thermal radiation is highly left-handed circularly polarized in all directions. The total optical helicity H is nonzero as,[29]

$$I = \sum_k \hbar \left(n_{k,\sigma+} - n_{k,\sigma-}\right) \propto \sum_k \left(\sigma_+ - \sigma_-\right) \tag{1}$$

where $n_{k,\sigma+}$ and $n_{k,\sigma-}$ are the photon numbers of LCP and RCP associated with the wavevector k. To explore the fundimental limit, we use a P parameter, defined as the optical helicity in percentage, normalized by the optical helicity of a emitter where the thermal radiation is perfectly LCP towards all directions. We show our design reaches P=39% of the fundamental limit from the experimental results. This is in strong contrast with previous demonstrations, where the spin characteristics are anti-symmetric in k-space ($n_{\sigma+}(k) = n_{\sigma-}(-k)$) because of the preservation of mirror symmetry, and the optical helicity has to sum to zero. We emphasize the breaking of mirror symmetry in the metasurface is the fundamental mechanism for this observation of non-zero optical helicity in the radiation excited by thermal fluctuations.

Symmetry Engineering

Moreover, we show in the following the photon spin characteristics are explicitly governed by the spatial symmetries. We emphasize that one distinctive feature of the 'F' structure is the complete symmetry breaking. None of the mirror symmetry, inversion symmetry, or rotational symmetry are present in the meta-atoms, which provides the full freedom for symmetry engineering. In other words, by introducing new symmetries, we find effective control of thermal radiation can be realized in its spectral, spatial, and especially spin properties. To show this, in Fig. 4, we present the $E-k$ dispersion along k_y ($k_x = 0$) of the averaged emissivity and the corresponding DoCP in three different metasurfaces with mirror, inversion, and 4-fold rotational symmetries (C4), respectively. We point out some interesting features in the obtained thermal emission spectra. Firstly, by introducing mirror-symmetry, the DoCP becomes zero, as the symmetry along y-axis guarantees DoCP = 0 at $k_x = 0$, regardless the value of k_y. Secondly, we show that the DoCP in the inversion-symmetric device becomes symmetric in the k-space, which is in strong contrast to the 'single-F' metasurface where the DoCP is asymmetric. Thirdly, the C4 device also exhibits symmetric patterns, as in 2D, the C4 symmetry contains the inversion symmetry (equivalent to C2). However, distinctive spectral, spatial, and spin features are present as a manifestation of the additional rotation symmetry. Reassuringly, all averaged emissivity plots show symmetric patterns in k-space, which guarantees the time-reversal symmetry is always preserved in our devices.

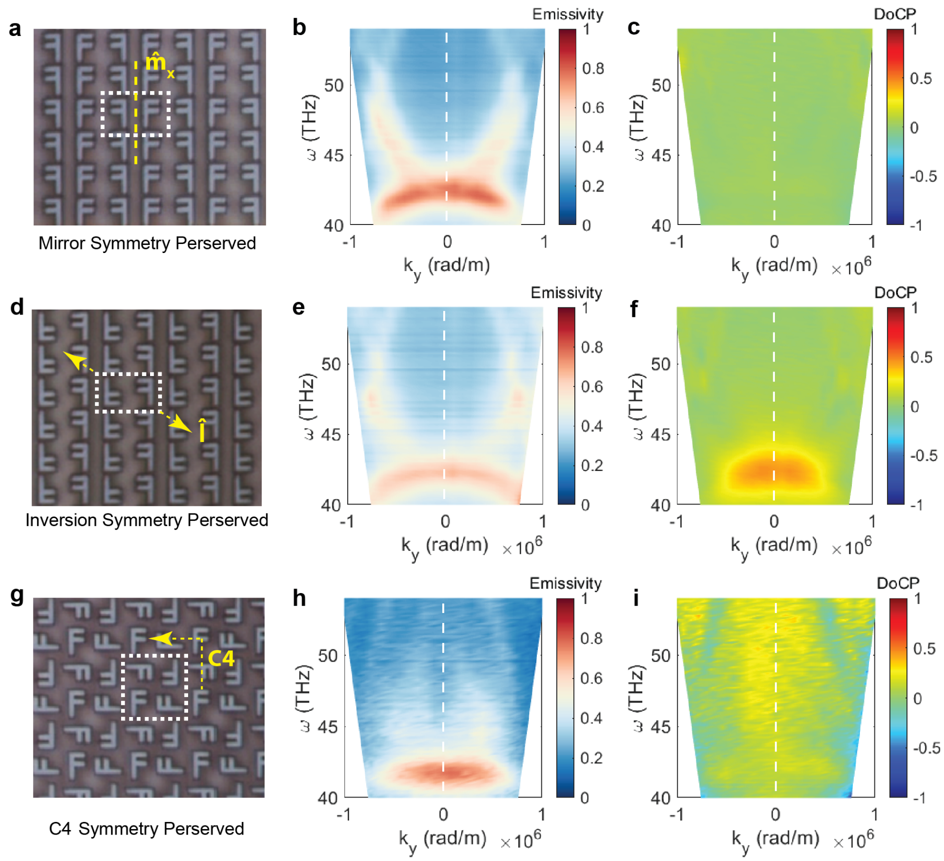

Figure 4: The optical images (left), averaged emissivity spectra (middle), and DoCP are plotted for devices with mirror symmetry (a-c), inversion symmetry (d-f), and four-fold rotational symmetry (g-i), respectively. The average emissivity is symmetric along k=0 in all three cases, which is a manifestation of the time-reversal symmetry. The DoCP is zero for the mirror-symmetric device, and symmetric for the inversion- and C4- devices.

Discussion

Finally, we discuss the impact and some potential applications of our results. First of all, the observed non-vanishing optical helicity indicates omnidirectional circularly polarized thermal emitters can be realized through metasurfaces. Our demonstrated devices can be directly applied as a wide-angle, narrow-band circular-polarized mid-infrared light source, for applications including optical gas sensing, illumination, and display. We highlight that the metasurface-based device can be integrated into on-chip systems to achieve compact functional devices for commercialization, while the current approach generally requires bulky optical components like linear polarizers and waveplates. Especially, traditional waveplate also suffers from the strong angular dependence, which makes omnidirectional circular polarization inaccessible. Moreover, considering the field of near-field heat transfer, we expect our designs can transfer net angular momentum and torque through heat, which may facilitate the discovery of novel phenomena at the nanoscale and benefit the development of near-field thermophotovoltaics. Additionally, the unique spectral-spatial-spin feature of the engineered thermal emission can be exploited as high-contrast thermal beacons for astronomy applications, as the thermal emission from other natural objects is highly incoherent, especially lack of spin textures. Finally, our symmetry-based strategy for controlling optical spin introduces a new degree of freedom of thermal radiation engineering, providing a general approach to comprehensively tailoring thermal radiation for future energy applications.

Data Availability

The data that supports this paper and other findings are available from the corresponding author on reasonable request.

Acknowledgments

The authors thank F. Kalhor for useful discussions. The authors thank A. Jishi for experimental assistance. The authors thank the Defense Advanced Research Projects Agency (DARPA) Nascent Light-Matter Interactions (NLM) for funding to pursue this research.

Competing Interests

The authors declare no competing interests.

References

(1) Baranov, D. G.; Xiao, Y.; Nechepurenko, I. A.; Krasnok, A.; Alù, A.; Kats, M. A. Nanophotonic engineering of far-field thermal emitters. *Nature materials* **2019**, *18*, 920–930.

(2) Fan, S. Thermal photonics and energy applications. *Joule* **2017**, *1*, 264–273.

(3) Lenert, A.; Bierman, D. M.; Nam, Y.; Chan, W. R.; Celanović, I.; Soljačić, M.; Wang, E. N. A nanophotonic solar thermophotovoltaic device. *Nat. Nanotechnol.* **2014**, *9*, 126–130.

(4) Bierman, D. M.; Lenert, A.; Chan, W. R.; Bhatia, B.; Celanović, I.; Soljačić, M.; Wang, E. N. Enhanced photovoltaic energy conversion using thermally based spectral shaping. *Nat. Energy.* **2016**, *1*, 16068.

(5) LaPotin, A.; Schulte, K. L.; Steiner, M. A.; Buznitsky, K.; Kelsall, C. C.; Friedman, D. J.; Tervo, E. J.; France, R. M.; Young, M. R.; Rohskopf, A., et al. Thermophotovoltaic efficiency of 40%. *Nature* **2022**, *604*, 287–291.

(6) Raman, A. P.; Anoma, M. A.; Zhu, L.; Rephaeli, E.; Fan, S. Passive radiative cooling below ambient air temperature under direct sunlight. *Nature* **2014**, *515*, 540–544.

(7) Mandal, J.; Fu, Y.; Overvig, A. C.; Jia, M.; Sun, K.; Shi, N. N.; Zhou, H.; Xiao, X.; Yu, N.; Yang, Y. Hierarchically porous polymer coatings for highly efficient passive daytime radiative cooling. *Science* **2018**, *362*, 315–319.

(8) Otey, C. R.; Lau, W. T.; Fan, S., et al. Thermal rectification through vacuum. *Physical review letters* **2010**, *104*, 154301.

(9) Ben-Abdallah, P.; Biehs, S.-A. Near-field thermal transistor. *Physical review letters* **2014**, *112*, 044301.

(10) Popa, D.; Udrea, F. Towards integrated mid-infrared gas sensors. *Sensors* **2019**, *19*, 2076.

(11) Asano, T.; Suemitsu, M.; Hashimoto, K.; De Zoysa, M.; Shibahara, T.; Tsutsumi, T.; Noda, S. Near infrared to visible highly selective thermal emitters based on an intrinsic semiconductor. *Sci. Adv.* **2016**, *2*, e1600499.

(12) Dyachenko, P. N.; Molesky, S.; Petrov, A. Y.; Störmer, M.; Krekeler, T.; Lang, S.; Ritter, M.; Jacob, Z.; Eich, M. Controlling thermal emission with refractory epsilon-near-zero metamaterials via topological transitions. *Nat. Commun.* **2016**, *7*, 11809.

(13) Yeng, Y. X.; Ghebrebrhan, M.; Bermel, P.; Chan, W. R.; Joannopoulos, J. D.; Soljačić, M.; Celanovic, I. Enabling high-temperature nanophotonics for energy applications. *Proc. Natl. Acad. Sci.* **2012**, *109*, 2280–2285.

(14) Liu, X.; Tyler, T.; Starr, T.; Starr, A. F.; Jokerst, N. M.; Padilla, W. J. Taming the Blackbody with Infrared Metamaterials as Selective Thermal Emitters. *Phys. Rev. Lett.* **2011**, *107*, 045901.

(15) De Zoysa, M.; Asano, T.; Mochizuki, K.; Oskooi, A.; Inoue, T.; Noda, S. Conversion of broadband to narrowband thermal emission through energy recycling. *Nature Photonics* **2012**, *6*, 535–539.

(16) Park, J. H.; Han, S. E.; Nagpal, P.; Norris, D. J. Observation of thermal beaming from tungsten and molybdenum bull's eyes. *ACS Photonics* **2016**, *3*, 494–500.

(17) Xu, J.; Mandal, J.; Raman, A. P. Broadband directional control of thermal emission. *Science* **2021**, *372*, 393–397.

(18) Bailey, J.; Chrysostomou, A.; Hough, J.; Gledhill, T.; McCall, A.; Clark, S.; Ménard, F.; Tamura, M. Circular polarization in star-formation regions: Implications for biomolecular homochirality. *Science* **1998**, *281*, 672–674.

(19) De, S.; Tashiro, H. Circular Polarization of the CMB: A probe of the First stars. *Physical Review D* **2015**, *92*, 123506.

(20) Maghrebi, M. F.; Gorshkov, A.; Sau, J. Fluctuation-induced torque on a topological insulator out of thermal equilibrium. *Physical review letters* **2019**, *123*, 055901.

(21) Khan, E.; Narimanov, E. E. Spinning radiation from a topological insulator. *Physical Review B* **2019**, *100*, 081408.

(22) Wang, Y.; Khandekar, C.; Gao, X.; Li, T.; Jiao, D.; Jacob, Z. Broadband circularly polarized thermal radiation from magnetic Weyl semimetals. *Optical Materials Express* **2021**, *11*, 3880–3895.

(23) Shitrit, N.; Yulevich, I.; Maguid, E.; Ozeri, D.; Veksler, D.; Kleiner, V.; Hasman, E. Spin-optical metamaterial route to spin-controlled photonics. *Science* **2013**, *340*, 724–726.

(24) Yin, X.; Ye, Z.; Rho, J.; Wang, Y.; Zhang, X. Photonic spin Hall effect at metasurfaces. *Science* **2013**, *339*, 1405–1407.

(25) Nalitov, A.; Malpuech, G.; Terças, H.; Solnyshkov, D. Spin-orbit coupling and the optical spin hall effect in photonic graphene. *Physical review letters* **2015**, *114*, 026803.

(26) Hentschel, M.; Schäferling, M.; Duan, X.; Giessen, H.; Liu, N. Chiral plasmonics. *Science advances* **2017**, *3*, e1602735.

(27) Hendry, E.; Carpy, T.; Johnston, J.; Popland, M.; Mikhaylovskiy, R.; Lapthorn, A.; Kelly, S.; Barron, L.; Gadegaard, N.; Kadodwala, M. Ultrasensitive detection and char-

acterization of biomolecules using superchiral fields. *Nature nanotechnology* **2010**, *5*, 783–787.

(28) Tang, Y.; Cohen, A. E. Optical chirality and its interaction with matter. *Physical review letters* **2010**, *104*, 163901.

(29) Cameron, R. P.; Barnett, S. M.; Yao, A. M. Optical helicity, optical spin and related quantities in electromagnetic theory. *New Journal of Physics* **2012**, *14*, 053050.